Elsevier Editorial System(tm) for Plant Physiology and Biochemistry

Manuscript Draft

Manuscript Number: PLAPHY-D-19-01930

Title: Energy conversion processes and related gene expression in a sunflower mutant with altered salicylic acid metabolism

Article Type: Research Paper

Keywords: Carboxylation efficiency; Electron transport rate; Light energy dissipation; Photosynthetic pigments; Plant hormones; Real-time Quantitative PCR

Corresponding Author: Dr. Andrea Scartazza, Ph.D.

Corresponding Author's Institution: Institute of Research on Terrestrial Ecosystems, Italy

First Author: Andrea Scartazza, Ph.D.

Order of Authors: Andrea Scartazza, Ph.D.; Marco Fambrini; Lorenzo Mariotti; Piero Picciarelli; Claudio Pugliesi

Abstract: Salicylic acid (SA) is involved in several responses associated with plant development and defence against biotic and abiotic stress, but its role on photosynthetic regulation is still under debate. This work investigated energy conversion processes and related gene expression in the brachytic mutant of sunflower lingering hope (linho), characterized by a higher ratio between the free SA form and its conjugate form SA O-β-D-glucoside (SAG) compared to wild type. The mutant showed an inhibition of photosynthesis, due to a combination of both stomatal and non-stomatal limitations. The reduced carboxylation efficiency was associated with a down-regulation of the gene expression for both the large and small subunits of Rubisco and the Rubisco activase enzyme. Moreover, linho showed an alteration of photosystem II (PSII) functionality, with reduced PSII photochemistry, increased PSII excitation pressure and decreased thermal energy dissipation of excessive light energy. These responses were associated with a lower photosynthetic pigments concentration and a reduced gene expression for light-harvesting chlorophyll a/b binding proteins (i.e. HaLhcA), chlorophyll binding subunits of PSII proteins (i.e. HaPsbS and HaPsbX) and phytoene synthase enzyme. The concomitant stimulation of respiratory metabolism, suggests that linho activated a coordinate modulation of chloroplast and mitochondria activities to compensate the energy imbalance and regulate energy conversion processes.

Dear Editor,

Please find enclosed the manuscript (research paper) "**Energy conversion processes and related gene expression in a sunflower mutant with altered salicylic acid metabolism**" by Andrea Scartazza, Marco Fambrini, Lorenzo Mariotti, Piero Picciarelli, Claudio Pugliesi

The study described in this manuscript investigated the energy conversion processes in a sunflower mutant (*lingering hope*, *linho*) characterized by a high ratio between the free Salicylic acid (SA) form and its conjugate form SA O-β-D-glucoside (SAG) compared to wild type. Salicylic acid is involved in several responses associated with plant development and defence against biotic and abiotic stress, but its role on the regulation of energy conversion processes and, especially, on photosynthesis is still under debate and there is a lack of information. Results show that the high SA/SAG ratio in *linho* was reflected in a coordinated modulation of energy conversion processes and related gene expression. Hence, this mutant constituted a great opportunity to study the effects of altered SA levels on photosynthetic performance and related gene expression under non-stress conditions.

We state that all the material is original and that no part has been published previously or submitted as a printed article elsewhere. All the authors have explicitly approved the submission of this manuscript.

Hoping that the manuscript will be suitable for publication in Your Journal, we send my best regards.

Thanks for Your attention.

Yours sincerely,

Andrea Scartazza[1] and Lorenzo Mariotti[2]

[1] Institute of Research on Terrestrial Ecosystems (IRET), National Research Council of Italy (CNR), Via Moruzzi 1, I-56124 Pisa, Italy; Tel. +39 050 6212469; Fax +39 050 6212473
E-mail address: andrea.scartazza@cnr.it (A. Scartazza)

[2] Department of Agriculture, Food and Environment (DAFE) University of Pisa, Via del Borghetto 80, I-56124 Pisa, Italy; Tel. +39 050 2216550; Fax +39 050 2216532
E-mail address: lorenzo.mariotti@unipi.it (L. Mariotti)

Graphical Abstract

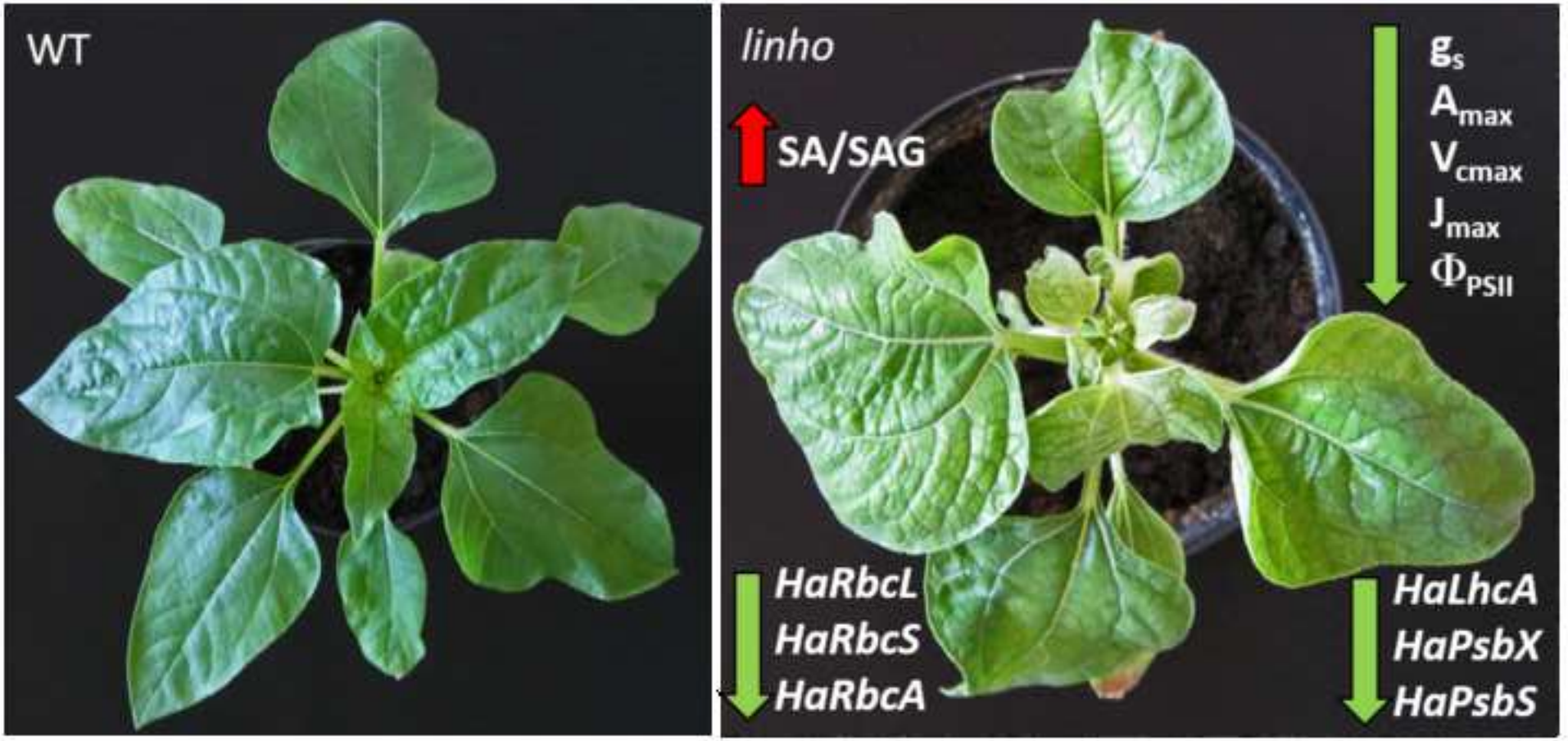

Highlights

Sunflower mutant *linho* showed high endogenous SA/SAG ratio in non-stress conditions

Photosynthesis in *linho* was inhibited by stomatal and non-stomatal constrains

linho showed an alteration of PSII functionality and light energy dissipation

Down-regulation of key photosynthetic-related genes was detected in *linho*

Data suggest a regulatory role of SA/SAG ratio on the energy balance of this mutant

Energy conversion processes and related gene expression in a sunflower mutant with altered salicylic acid metabolism

Andrea Scartazza[*,1], Marco Fambrini[2], Lorenzo Mariotti[*,2], Piero Picciarelli[2], Claudio Pugliesi[2]

Running title: Photosynthesis in a sunflower mutant with high SA/SAG ratio

[1] *Institute of Research on Terrestrial Ecosystems (IRET), National Research Council (CNR), Via Moruzzi 1, I-56124, Pisa, Italy*

[2] *Department of Agriculture, Food and Environment (DAFE) University of Pisa, Via del Borghetto 80, I-56124 Pisa, Italy*

* Corresponding author at: *Institute of Research on Terrestrial Ecosystems (IRET), National Research Council (CNR), Via Moruzzi 1, I-56124, Pisa, Italy*

E-mail address: andrea.scartazza@cnr.it (A. Scartazza)

* Corresponding author at: *Department of Agriculture, Food and Environment (DAFE) University of Pisa, Via del Borghetto 80, I-56124 Pisa, Italy*

E-mail address: lorenzo.mariotti@unipi.it (L. Mariotti)

Orcid Numbers

Andrea Scartazza: 0000-0001-5048-5112

Lorenzo Mariotti: 0000-0002-3152-1867

Piero Picciarelli: 0000-0002-2372-0620

Claudio Pugliesi: 0000-0001-5846-7947

ABSTRACT

Salicylic acid (SA) is involved in several responses associated with plant development and defence against biotic and abiotic stress, but its role on photosynthetic regulation is still under debate. This work investigated energy conversion processes and related gene expression in the brachytic mutant of sunflower *lingering hope* (*linho*), characterized by a higher ratio between the free SA form and its conjugate form SA O-β-D-glucoside (SAG) compared to wild type. The mutant showed an inhibition of photosynthesis, due to a combination of both stomatal and non-stomatal limitations. The reduced carboxylation efficiency was associated with a down-regulation of the gene expression for both the large and small subunits of Rubisco and the Rubisco activase enzyme. Moreover, *linho* showed an alteration of photosystem II (PSII) functionality, with reduced PSII photochemistry, increased PSII excitation pressure and decreased thermal energy dissipation of excessive light energy. These responses were associated with a lower photosynthetic pigments concentration and a reduced gene expression for light-harvesting chlorophyll *a*/*b* binding proteins (*i.e.* HaLhcA), chlorophyll binding subunits of PSII proteins (*i.e.* HaPsbS and HaPsbX) and phytoene synthase enzyme. The concomitant stimulation of respiratory metabolism, suggests that *linho* activated a coordinate modulation of chloroplast and mitochondria activities to compensate the energy imbalance and regulate energy conversion processes.

Keywords:

Carboxylation efficiency

Electron transport rate

Light energy dissipation

Photosynthetic pigments

Plant hormones

Real-time Quantitative PCR

Abbreviations

A	Steady-state photosynthetic CO_2 assimilation rate
A_{max}	Light saturated rate of photosynthesis at growth CO_2 concentration
AQY	Apparent quantum yield
C_i	Intercellular CO_2 concentration
Car	Total carotenoids
CCP	CO_2 compensation point
Chl*a*	Chlorophyll *a*
Chl*b*	Chlorophyll *b*
Θ	Convexity factor of the photosynthetic light curve
E	Transpiration rate
F_v/F_m	Potential efficiency of PSII photochemistry
Φ_{PSII}	Actual photon yield of PSII photochemistry
GC-MS/MS	Gas Chromatography tandem Mass Spectrometry
g_s	Stomatal conductance
HaFNR	*Ferredoxin-NADP + reductase*
HaLhcA	*Photosystem I chlorophyll a/b-binding protein 3-1, chloroplastic*
HaPsbS	*Photosystem II 22 kDa protein*
HaPsbX	*Photosystem II PsbX*
HaPSY	*Phytoene synthase*
HaRbcA	*Ribulose bisphosphate carboxylase/oxygenase activase*
HaRbcL	*RuBisCO large subunit*
HaRbcS	*RuBisCO small subunit*
HaVDE	*Violaxanthin de-epoxidase*
J_{max}	Maximum light-driven electron transport rate
LI-COR	LI-6400-40 portable photosynthesis system
linho	*lingering hope*
NPQ	Non-photochemical quenching
PPFD	Photosynthetic photon flux density
R_D	Respiration rate in the dark
R_L	Respiration rate in the light
RT-qPCR	Real-time Quantitative PCR
SA	Salicylic acid

SAG	SA 2-O-β-D-glucoside
Vc_{max}	Maximum carboxylation rate
$1-F_v'/F_m'$	Fraction of thermal dissipation in PSII
$1-q_p$	Excitation pressure at PSII

1. Introduction

The study of plant metabolism and photosynthesis has benefited from isolation and characterization of spontaneous and/or induced mutants in plant models and crops (Levine, 1969; Thorneycroft et al., 2001; Rochaix 2004; Slattery et al., 2017). Foyer et al. (2012) suggested that photosynthetic control operates at multiple levels to balance energy supply and energy demand to optimize the photosynthetic efficiency. This requires the involvement of a complex network of forward and retrograde signalling pathways which acts, in response to environmental and metabolic changes, on both short-term post-translational modifications and longer-term regulation through coordinate gene expression in different cell compartments (chloroplasts, mitochondria and nuclei). Among the metabolic factors involved in the photosynthetic control, a fundamental role is played by the hormone signals. Salicylic acid (SA) is an important plant hormone involved in several responses associated with plant development and defence against biotic and abiotic stress (Maruri-López et al., 2019; Zhang and Li, 2019), but its role on the regulation of photosynthesis is still under debate (Rivas-San Vicente and Plasencia, 2011; Kumar, 2014; Gao et al., 2018; Lu and Yao 2018; Dogra and Kim 2019; Poór et al., 2019). In fact, notwithstanding several studies have examined the photosynthetic responses of exogenously SA-treated plants, it is not still clear if these responses are due to stomatal or non-stomatal factors (Janda et al., 2014; Handa et al., 2017). In addition, the effects of SA on photosynthesis is strongly dependent on species and SA doses, with low doses that generally have a beneficial effect and high doses that cause a photosynthetic depression (Rivas-San Vicente and Plasencia, 2011). However, it is controversial if the reduced photosynthetic capacity in plants treated with high SA concentration is a direct effect of SA on the photosynthetic metabolism or a secondary response caused by the partial stomatal closure that induces an increased excitation pressure at PSII, leading to ROS formation and injuries at the photosynthetic apparatus (Janda et al., 2012; 2014). Anyway, these studies suggested that controlled

SA concentration plays a key role for optimal photosynthetic performance and for acclimation to changing environmental stimuli (Mateo et al., 2006; Janda et al., 2014).

Mutants or transgenic plants with constitutively high SA level represent key tools to understand the direct effects of genetically varied SA concentration on growth, photosynthesis and defence responses. The characterization of SA-over-accumulating mutants of *Arabidopsis thaliana* directly demonstrated that SA controls different aspects of plant growth, including photosynthesis (Janda et al., 2014). Mutants of *Arabidopsis* with high SA content, such as *cpr1-1*, *cpr5-1*, *cpr6-1* or *dnd1-1*, are dwarf and exhibit an altered photosynthetic activity under non-stress conditions (Mateo et al., 2006). In particular, these mutants showed reduced values of stomatal conductance, CO_2 assimilation rate and quantum yield of PSII photochemistry, associated with higher dark respiration and thermal energy dissipation capacity (Janda et al., 2014). Recently, mutants and transgenic lines of *Arabidopsis* with alteration of SA levels have been investigated under cadmium-induced stress. The reduced basal SA level in *nahG* plants was associated with the acclimation of photosynthetic apparatus under cadmium stress, while the opposite responses were observed in the high SA-accumulating mutant *snc1* (Wang et al., 2019). Photosynthetic performance of the *sid2-1* mutant of *Arabidopsis*, with a low SA endogenous level, has been studied in the acclimation of plants to a combination of heat stress and drought (Kumazaki and Suzuki, 2019). Moreover, decreasing levels of endogenous SA delayed onset of senescence with an extension of the photosynthetic period and a change of resource allocation, contributing to the development of heterosis (Groszmann et al., 2015; Gonzalez-Bayon et al., 2019). An altered photosynthetic performance was also observed in transgenic plants of *Populus tremula* × *alba* with constitutively elevated SA level, which exhibited significantly reduced net photosynthesis, stomatal conductance and transpiration rate relative to the wild type (WT) under high temperature growth (Xue et al., 2013). However, these authors, conversely to what reported for the *Arabidopsis* mutants, did not observe a significant effect of high SA level on growth, possibly due to the high photosynthetic capacity of this species and the metabolic flexibility afforded by the dynamic chlorogenic acids pool.

Recently, a brachytic mutant of sunflower with altered SA metabolism (*lingering hope*, *linho*) has been isolated and characterized (Mariotti et al., 2018). This mutant showed abnormal growth of leaves, petioles, stem internodes and capitula. In addition, young *linho* plants showed frequently chlorosis especially in the proximal end of leaves, whereas at reproductive stage *linho* leaves showed alteration of leaf width/length ratio, asymmetric shape and undersized lamina curled downwards in upper nodes (Mariotti et al., 2018). At early stage of growth, SA content of *linho* leaves was higher than WT starting from the second node and, interestingly, the very high SA level in the upper node leaves at reproductive stage depended on a drastic reduction of the conjugate SA 2-O-β-D-glucoside (SAG) level. Therefore, *linho* mutant showed an alteration of endogenous SA/SAG ratio under non-stress conditions and a different pattern of gene expression for two pathogenesis-related genes and two genes involved in SA biosynthesis and metabolism (Mariotti et al., 2018). In addition, these authors showed that the reduced growth and internode elongation in *linho* mutant was associated with an inhibition of photosynthetic performance, although it was not clear if this photosynthetic limitation was mainly due to stomatal or non-stomatal constrains and which genes were involved in this response. On the other hand, this information is essential to understand the role of endogenous SA in regulating photosynthesis and redox state in higher plants under non-stress conditions.

The main aims of this work were: i) to unravel the stomatal and non-stomatal factors affecting photosynthetic performance and energy conversion processes in *linho* mutant by combining gas exchanges, fluorescence measurements and pigment analysis; ii) to evaluate the role of photosynthetic related genes involved in these responses through gene expression analysis by reverse transcription-quantitative real-time polymerase chain reaction (RT-qPCR).

2. Material and methods

2.1. Plant material and growth conditions

Sunflower seeds of WT and *linho* mutant were germinated in Petri dishes on distilled water. Germination took place in a growth chamber in the dark at 23 ± 1 °C. After 3 days, the germinated seeds were transplanted into small plastic pots (50 mL) containing a mixture of soil and sand. Two weeks later, the seedlings were transplanted into larger pots (3 L) containing the same substrate but plus an initial dose of complete fertilizer (Osmocote® 14-14-14; Scotts, Marysville, OH, USA) and grown until anthesis. Growth conditions were 25 ± 1 °C and 16 h photoperiod. Irradiation was 200 μmol m^{-2} s^{-1} (photosynthetic photon flux density, PPFD) provided from a mixture of cool-white fluorescent (Philips TLD 30W/33, Philips, Eindhoven, The Netherlands) and mercury-vapour HPI-T 400 W (Philips) lamps. Chemical treatments for preventive plant protection were practised.

2.2. Hormonal analyses

Analysis of endogenous hormones was in agreement with Mariotti et al. (2018). Briefly, approximately 1,000 mg of leaf fresh material, collected from the second pair of leaves of 21-old-plants in both WT and *linho*, were homogenized in cold 80% (v/v) methanol (1:5, w/v) using a microdevice. [$^2H_4$]-SA (CDN Isotopes Inc., Quebec, Canada) was added as internal standards to account for purification losses. Methanol was evaporated under vacuum at 35 °C and the aqueous phase was partitioned against ethyl acetate, after adjusting the pH to 2.8. The extracts were dried and resuspended in 0.3-0.5 mL of water with 0.01% acetic acid and 10% methanol. HPLC analysis was performed with a Kontron instrument (Munich, Germany) equipped with a UV absorbance detector operating at 214 nm. The samples were applied before to 150 × 4.6 mm ID. ODS Hypersil (Thermo) particle size 5 μm were eluted at a flow rate of 1 mL min^{-1}. The column held constant at 10% MeOH for 5 min of the run, followed by a double gradient elution from 10% to 30% and 30% to 100% over 20 min. The fractions corresponding to the elution volumes of standard hormones were collected separately. The fractions were dried and silylated with N,Obis (trimethylsilyl)

trifluoroacetamide containing 1% trimethylchlorosilane (Pierce, Rockford, IL, USA) at 70 °C for 1 h. Chromatography-tandem mass spectrometry (GC-MS/MS) analysis was performed on a Saturn 2200 quadrupole ion trap mass spectrometer coupled to a CP-3800 gas chromatograph (Varian Analytical Instruments, Walnut Creek, CA, USA) equipped with a MEGA 1MS capillary column (30 m × 0.25 mm i.d., 0.25 μm film thickness) (Mega, Milano, Italy). The carrier gas was helium, which was dried and air free, with a linear speed of 60 cm s^{-1}. The oven temperature was maintained at 80 °C for 2 min and increased to 300 °C at a rate of 10 °C min^{-1}. Injector and transfer line were set at 250 °C and the ion source temperature at 200 °C. Full scan mass spectra were obtained in EI + mode with an emission current of 10 μA and an axial modulation of 4 V. Data acquisitions was from 100 to 600 Da at a speed of 1.4 scan s^{-1}. Final data were the means of three biological replicates. SA and SAG were identified by comparison of full mass spectra with those of authentic compounds. Quantification was carried out by reference to standard plots of concentration ratios versus ion ratios, obtained by analysing known mixtures of unlabelled and labelled SA.

2.3. Pigment analysis

Pigment extraction for spectrophotometric analysis was performed as previously described (Fambrini et al., 2004) on leaves of WT and *linho* plants grown in growth chamber. The analyses were carried out on leaves of both second pair of 21-day-old plants and of the 11°-12° internode of 70-day-old plants. Ten extracts were obtained for each genotype, and two measurements were made per extract.

2.4. Gas exchange and fluorescence measurements

Gas exchange and fluorescence measurements were performed using the LI-6400-40 portable photosynthesis system (LI-COR) equipped with the leaf chamber fluorometer. Measurements were

performed on the second pairs of leaves of WT and *linho* plants at vegetative stage (21-days-old plants) and on fully-expanded leaves of the 11°-12° internode at reproductive stage (70-days-old plants). All the measured parameters were expressed as the average of the measurements made on at least three fully expanded leaves for three individual experiments.

At vegetative stage, instantaneous measurements of steady-state photosynthetic CO_2 assimilation rate (A), stomatal conductance (g_s), intercellular CO_2 concentration (C_i), transpiration rate (E), actual photon yield of PSII photochemistry (Φ_{PSII}), Stern–Volmer non-photochemical quenching (NPQ) and the potential efficiency of PSII photochemistry (F_v/F_m) were performed between 09:00 and 11:00 h under growing PPFD (200 μmol m^{-2} s^{-1}), CO_2 concentration of 400 μmol mol^{-1} and leaf temperature of 25 °C, as reported in Scartazza et al. (2017). Measurements of F_v/F_m were determined after at least 30 min of leaf acclimation to dark. Actual photon yield of PSII photochemistry in the light was determined for each PPFD value as $\Phi_{PSII} = (F_m' - F_s)/F_m'$ (Genty et al., 1989) at steady state, where F_m' is the maximum fluorescence yield with all PSII reaction centres in the reduced state obtained superimposing a saturating light flash during exposition to actinic light and F_s is the fluorescence at the actual state of PSII reaction centres during actinic illumination. Non-photochemical quenching was determined according to the Stern–Volmer equation as $NPQ = (F_m/F_m') - 1$, where F_m is the maximum fluorescence yield in the dark. The actual reduction state of PSII reaction centres was calculated as $1 - q_p = (F - F_o')/(F_m' - F_o')$, where q_p represents the photochemical quenching and F_o' is the fluorescence yield with all reaction centres open in the presence of quenching. The fraction of light absorbed in PSII antennae that is dissipated thermally was estimated as $1\text{-}F_{v'}/F_{m'}$ (Demmig-Adams et al., 1996). The potential efficiency of PSII photochemistry was calculated on dark adapted leaves as $F_v/F_m = (F_m - F_o)/F_m$, where F_o is the minimal fluorescence yield emitted by the leaves in the dark-adapted state.

The A/C_i curves were performed on one of the second pair of leaves for each plant over a range of CO_2 concentration between 50 and 2500 μmol mol^{-1} at saturating PPFD values (1800 μmol

m^{-2} s^{-1}). Each step comprised ~5 min for adjustment and stabilization of the gas exchange parameters. Values of CO_2 compensation point (CCP), maximum carboxylation rate (Vc_{max}) and maximum light-driven electron transport rate (J_{max}) were estimated by fitting the mechanistic model of CO_2 assimilation proposed by Farquhar et al. (1980) to individual A/C_i response data. When necessary, measurements were corrected to 25 °C using the temperature responses of Bernacchi et al. (2001) and Bernacchi et al. (2003) for the ribulose-1,5-bisphosphate carboxylase-oxygenase (Rubisco) and RuBP-limited portions of the A/C_i curves, respectively.

Light response curves of gas exchange and fluorescence parameters were performed on the same leaves over a range of PPFD between 25 and 1800 μmol m^{-2} s^{-1}. Leaves were allowed to adapt to each irradiance level for ~10 min for adjustment and stabilization of the gas exchange and fluorescence parameters (steady-state values). Experimental data were fit using a non-rectangular empirical function to estimate the apparent quantum yield (AQY), the convexity factor of the curve (Θ) and the light saturated rate of photosynthesis at growth CO_2 concentration (A_{max}).

The respiration rate in the dark (R_D) and in the light (R_L) of the second pair of leaves were determined using the Kok method (Kok, 1948). Briefly, A was measured in a range of PPFD between 0 and 120 μmol m^{-2} s^{-1}, which generated a Kok break point at approximately 20 μmol m^{-2} s^{-1}. R_D and R_L were estimated by extrapolating to 0 PPFD the linear relationship between A and PPFD over the range 0-20 μmol m^{-2} s^{-1} PPFD and 20-120 μmol m^{-2} s^{-1} PPFD, respectively.

At reproductive stage (70-days-old plants), instantaneous measurements of gas exchange (A, g_s, C_i and E) and fluorescence (Φ_{PSII}, $1-q_p$, NPQ and $1-F_{v'}/F_{m'}$) parameters were carried out as described above on leaves of the 11°-12° internode at both growth (200 μmol m^{-2} s^{-1}) and saturating (1800 μmol m^{-2} s^{-1}) PPFD. The values of F_v/F_m and R_D were obtained after dark acclimation of the leaves for at least half an hour.

2.5. Gene expression analysis by reverse transcription-quantitative real-time polymerase chain reaction (RT-qPCR)

Expression analysis by RT-qPCR was performed for genes of sunflower implicated in: (i) carotenoid biosynthesis [*Phytoene synthase* (*HaPSY*)]; (ii) carbon fixation [*RuBisCO large subunit* (*HaRbcL*), *RuBisCO small subunit* (*HaRbcS*) and *Ribulose bisphosphate carboxylase/oxygenase activase* (*HaRbcA*)]; (iii) organization and functionality of the PSII and PSI [*Photosystem II PsbX* (*HaPsbX*), *Photosystem II 22 kDa protein* (*HaPsbS*), *Photosystem I chlorophyll a/b-binding protein 3-1, chloroplastic* (*HaLhcA*) and *Ferredoxin-NADP + reductase* (*HaFNR*)]; and (iv) complexes involved in the non-radiative (heat) dissipation of energy in the antennae [*Violaxanthin de-epoxidase* (*HaVDE*)]. The GenBank accession numbers, the gene-specific primers used for this analysis and the amplicon size are reported in Table S1.

Total RNA was extracted from leaves of the second pair of WT and *linho* plants with the TriPure Isolation Reagent, according to the manufacturer's instructions (Roche Diagnostics GmbH, Mannheim, Germany). Total RNA was treated with DNase I-RNase free (AMPD1-1KT), according to the manufacturer's instructions (Sigma Aldrich, St. Louis, MO, USA) and retro-transcribed with the iScript^{TM} cDNA synthesis kit, according to the manufacturer's instructions (Bio-Rad Laboratories S.r.l., Segrate, Milan, Italy).

Expression analysis was conducted using a Real-time Step One (Applied Biosystem, Thermo Fisher Scientific Inc., Waltham, MA, USA) and gene-specific primers (Table S1). Quantitative PCR was performed using 12.5 ng of cDNA and SYBR Green Master Mix (Thermo Fisher Scientific Inc.), according to the manufacturer's instructions. The thermal cycling conditions of RT-qPCR were as follows: 95 °C for 20 sec; 40 cycles (95 °C 3 sec, 57 or 58 °C 30 sec); Melt curve: 95 °C 15 sec/60 °C 60 sec/95 °C 15 sec. Relative quantification of specific mRNA levels was performed using the comparative $2^{-\Delta\Delta C}$T method (Livak and Schmittgen, 2001). Briefly, the C_T values of the amplified regions in all samples were normalized with the C_T values of the reference housekeeping

gene *18S* mRNA to eliminate the variations caused by sample handling. In addition, mRNAs from WT were used as reference sample. Melt-curve analyses were performed after the PCR. A single distinct peak was observed for each target (*HaPSY*, *HaRbcL, HaRbcS, HaRbcA, HaPsbX, HaLhcA, HaFNR, HaPsbS* and *HaVDE*) and control (*Ha18S*) gene indicating the specific amplification of a single product. *Ha18S* was used as the reference gene based on preliminary data that revealed consistent expression levels regardless of this organ type. In particular, the *Ha18S* was preferred after comparison with other putative housekeeping genes (Mariotti et al., 2018). The data were the average from three/four biological replicates, with each including three technical replicates. The software Real-time Step One v2.3, provided with the instrument by which we carried out the RT-qPCR, was used.

2.6. Statistical analysis

Statistical analysis was performed using the STATISTICA software package (StatSoft for Windows, 1998, Tulsa, OK, USA). Leaf pigments, hormonal content, gas exchange and fluorescence data were expressed as means ± SE from three independent experiments, with samples run in triplicates (plants). Differences between means were tested using the Student's t-test and indicated with * $P < 0.05$, ** $P < 0.01$ or * $P < 0.001$ in Tables 1-2 and Fig. 1. For RT-qPCR, the data ± SD were shown as an average expression value in the three/four biological replicates relative to that in the control sample that was set as one. Student's *t*-test was performed to analyse the differences in gene expression between WT and *linho* and indicated with * $P < 0.05$ or ** $P < 0.01$ in Fig. 5.

3. Results

3.1. Endogenous SA and SAG levels

The endogenous levels of free SA and its predominant inactive conjugate, SA 2-O-β-D-glucoside (SAG), have been determined at vegetative stage on the second pair of leaves (stage V6; Schneiter and Miller 1981) in 21-day-old plants of both *linho* and WT (Fig. 1). Leaf SA content in *linho* was about the double of that observed in WT, whereas SAG showed an opposite trend with a significant higher level in WT compared to the mutant. Consequently, SA + SAG content was not significantly different between *linho* and WT, while SA/SAG ratio dramatically increased in *linho* mutant (4.23 ± 0.79) with respect to WT (0.59 ± 0.02) (insert of Fig. 1).

3.2. Photosynthetic pigments, gas exchanges and energy dissipation processes at vegetative stage

The second pair of leaves in 21-day-old plants showed a lower content of both Chl *a* and Chl *b* in *linho* with respect to WT (Table 1). The total carotenoids content was also lower in *linho* than WT, although the difference was not statistically significant (Table 1). Plants of *linho* showed significantly lower values of CO_2 assimilation rate, stomatal conductance and transpiration rate than WT, while the intercellular CO_2 concentration was not significantly affected (Table 1). Moreover, both maximum and effective quantum yield of PSII photochemistry were significantly reduced in plants of *linho*, while the excitation pressure at PSII ($1-q_p$) increased without a significant increase in non-photochemical quenching (NPQ) and $1-F_{v'}/F_{m'}$ (Table 1).

Photosynthetic response of CO_2 assimilation rate to increasing photosynthetic photon flux density (PPFD) in the second pair of leaves of WT and *linho* plants are shown in Fig. 2. The mutant exhibited a lower initial slope of the curve and a lower maximum photosynthetic CO_2 uptake at saturating light intensity than WT. The apparent quantum yield (AQY) and the maximum CO_2 assimilation rate at saturating light intensity (A_{max}) were significantly lower in *linho* than WT, while no significant differences were observed for the convexity factor (Θ) (Table 1). The photosynthetic response of CO_2 assimilation rate to increasing intercellular CO_2 concentration (C_i) in the second

pair of leaves of *linho* and WT are reported in Fig. 3. The mutant showed a lower initial slope and a lower CO_2 assimilation rate at saturating CO_2 concentration than WT. Hence, *linho* was characterized by significantly lower values of both Vc_{max} and J_{max} than WT, although the J_{max}/Vc_{max} ratio and the CO_2 compensation point (CCP) did not show any significant variation (Table 1). The dark respiration rate (R_D) of the second pair of leaves was not significantly different between *linho* and WT, whereas the respiration rate in the light (R_L) and the R_L/R_D ratio were significantly higher in the mutant than WT (Table 1).

The light response curves of the fluorescence parameters (Φ_{PSII}, $1\text{-}q_p$ and NPQ) are reported in Fig. 4. Both WT and *linho* showed a decrease of Φ_{PSII} associated with an increase of $1\text{-}q_p$ and NPQ with increasing light irradiance. However, *linho* showed a lower Φ_{PSII} at all the PPFD values compared to WT (Fig. 4A). An opposite behavior was observed for $1\text{-}q_p$, with *linho* showing higher values than WT starting from 200 μmol m^{-2} s^{-1} of PPFD (Fig. 4B). Interestingly, NPQ showed a different behavior at relatively low and high PPFDs, respectively. In detail, at PPFDs ranging from 0 to about 200 μmol m^{-2} s^{-1}, *linho* showed slight higher values of NPQ than WT, whereas at PPFDs over 600 μmol m^{-2} s^{-1} the NPQ values were much higher in WT and the difference became even greater with as increased PPFD (Fig. 4C). In addition, the fraction of thermal dissipation in PSII, estimated as $1\text{-}F_{v'}/F_{m'}$, was higher in WT compared to *linho* at saturating light intensity (Table 1). Hence, the light-saturated value of Φ_{PSII}, $1\text{-}q_p$, NPQ and $1\text{-}F_{v'}/F_{m'}$ were significantly different between *linho* and WT (Table 1).

3.3. Gene expression analyses at vegetative stage

To evaluate if the altered photosynthetic performance of the mutant was associated with changes in the gene expression, we analyzed by RT-qPCR some photosynthetic-related genes of sunflower on the same second pair of leaves used for the photosynthetic analyses (Table S1). A

down-regulation of *Rubisco large subunit* (*HaRbcL*), *Rubisco small subunit* (*HaRbcS*), *Rubisco activase* (*HaRbcA*), *Photosystem II PsbX* (*HaPsbX*), *Photosystem II 22 kDa protein* (*HaPsbS*), *Photosystem I chlorophyll a/b-binding protein* (*HaLhcA*) and *Phytoene synthase* (*HaPSY*) genes was observed in *linho* with respect to WT (Fig. 5). Conversely, the gene expressions of *Ferredoxin-$NADP^+$ reductase* (*HaFNR*) and *Violaxanthin de-epoxidase* (*HaVDE*) were not significantly affected by the mutation (Fig. 5).

3.4. Photosynthetic pigments, gas exchanges and energy dissipation processes at reproductive stage

The effects of mutation on the photosynthetic performance of adult plants was evaluated by the determination of photosynthetic pigments concentration and measurements of gas exchange and chlorophyll fluorescence at reproductive stage (70-days-old plants, Table 2). Leaves of *linho* showed significantly lower concentrations of both chlorophylls and carotenoids compared to WT. The depigmented phenotype was associated with significantly lower values of A, g_s, E, Φ_{PSII} and F_v/F_m in *linho* at both growth and saturating light intensity. Conversely, *linho* showed significantly higher values of C_i, 1-q_p and R_D compared to WT. Finally, NPQ and 1-$F_{v'}/F_{m'}$ were not significantly different at growth light intensity, whereas at saturating light intensity they were significantly higher in WT than *linho*.

4. Discussion

4.1. Alteration of SA/SAG ratio in leaves

It has been suggested that SA levels play a key role for optimal photosynthetic performance and for acclimation to changing environmental stimuli (Janda et al., 2014). This hormone can be

conjugated in the cytoplasm to SAG and then actively transported into the vacuole where it may function as an inactive storage form able to release free SA (Dean and Mills, 2004; Maruri-López et al., 2019). Hence, the higher SA/SAG ratio in leaves of *linho* suggested an increase of acting free SA form in the mutant, without affecting the total pool. This result is in good agreement with that reported in the same mutant at reproductive stage (Mariotti et al., 2018) and indicates that, independently by the developmental stage and the amount of total SA, *linho* shows an alteration of the SA metabolism with an increased level of its free form into the leaves.

4.2. Effects of mutation on pigments concentration and photosynthetic performance

In the *linho* mutant, we found a reduced amount of photosynthetic pigments at both vegetative and reproductive stage, according to previous results (Mariotti et al., 2018). However, in this study, Chl *a* and Chl *b* showed a similar decrease in the mutant, hence the Chl *a*/Chl *b* ratio was only slightly affected. Previous findings reported that exogenous treatments with high SA concentrations induced a reduction in both chlorophyll and carotenoid contents (Çag et al., 2009; Habibi and Vaziri, 2017) and a change of the chloroplast ultrastructure (Uzunova and Popova, 2000; Poór et al., 2019), suggesting an effect of SA on the thylakoid membranes (Rivas-San Vicente and Plasencia, 2011; Janda et al., 2014). Interestingly, the reduced pigment concentration in *linho* was associated with a down-regulation of the genes encoding for both light-harvesting chlorophyll *a*/*b* binding proteins (*i.e.* HaLhcA) and chlorophyll binding subunits of PSII proteins (*i.e.* HaPsbS and HaPsbX), indicating a structural alteration of the chlorophyll-protein complexes implicated in light capture and PSII functionality. Plants of *linho* showed a reduction of A, g_s and Φ_{PSII} in the second pair of leaves without significant changes in C_i, as previously observed (Mariotti et al., 2018). Similar results were found in adult plants, although at reproductive stage *linho* leaves showed significant higher C_i values than WT at both growth and saturating light intensity. These results highlighted that the partial stomatal closure restricted entry of CO_2 into substomatal spaces limiting

CO_2 assimilation, but the unchanged (at vegetative stage) or increased (at reproductive stage) C_i with reduced Φ_{PSII} revealed that CO_2 was not efficiently consumed by the plants. This suggests that the inhibition of photosynthesis in *linho* occurred due to both the reduced CO_2 diffusion into the leaf and the decreased efficiency of carbon assimilation. Our results agree with previous findings on several *Arabidopsis* SA mutants (Mateo et al., 2006), where growth retardation in plants with constitutively high SA levels was explained by decreased F_v/F_m, Φ_{PSII} and g_s, although these authors did not investigate the causes of such effects.

4.3. Light and CO_2 dependent photosynthetic limitation

Light and CO_2 photosynthetic response curves were carried out at vegetative stage to unravel the non-stomatal factors affecting the reduced photosynthetic performance of *linho*. The photosynthetic light-response curves showed significant differences between WT and *linho* at both low and high irradiances, leading to lower AQY and A_{max} values in the mutant. At low irradiances, photosynthesis is limited by the rate of electron transport, while at high irradiances photosynthesis is frequently limited by the Rubisco activity. The initial slope of the CO_2 response curves clearly indicated a reduction of the maximum carboxylation efficiency of Rubisco (*i.e.* reduced Vc_{max}) in *linho* plants. In addition, the mutant showed a lower maximum photosynthesis rate at saturating CO_2 compared to WT, which is related to limited ribulose biphosphate (RuBP) regeneration and, hence, to an inhibition of the maximum photosynthetic electron transport rate (*i.e.* reduced J_{max}). Interestingly, the reduced photosynthetic rate in *linho* was associated with unchanged J_{max}/Vc_{max} ratio, suggesting a balance between RuBP carboxylation and RuBP regeneration photosynthetic limitations. Controversial results were observed with exogenous treatments with SA on Rubisco, depending on the species and SA concentration (Janda et al., 2014). In barley plants, the Rubisco activity decreased while the activity of phosphoenolpyruvate carboxylase (PEPC) increased with increasing SA concentrations (Pancheva et al., 1996). Conversely, low doses of exogenous SA have

been associated with an up-regulation of carboxylation efficiency (Fariduddin et al., 2003). Rubisco is composed of eight large subunits containing the active site and eight small subunits that are required for maximal catalysis and, in several cases, for CO_2/O_2 specificity (Andersson, 2008). Our data showed a significant reduction of Vc_{max} associated with a down-regulation of genes encoding for both large (*HaRbcL*) and small (*HaRbcS*) subunits in *linho* mutant, although the small subunit gene was more down-regulated than the large subunit one. Accordingly, Pancheva and Popova (1998) showed a decrease of about 50% in the level of Rubisco in barley leaves treated with 1 mmol L^{-1} SA compared to control plants, demonstrating that high SA levels inhibited the synthesis of both Rubisco subunits and, especially, the small ones. A proteomic study carried out by Wu et al. (2013) in maize leaves showed that the two protein spots of the SA responsive protein, Rubisco large subunit, exhibited opposite expression patterns at protein level: one protein spot was up-regulated while the other was down-regulated. The authors explained this phenomenon hypothesizing that the same protein in maize leaves may have different isoforms characterized by contrasting roles under phytohormone stress (Wu et al., 2013). In addition, the Rubisco activase enzyme (RbcA) also regulates the carboxylation efficiency (Portis et al., 2007). The *Rubisco activase* (*HaRbcA*) gene was down-regulated in *linho*, suggesting that the reduced carboxylation efficiency in this mutant was due to changes in both structure and activation state of the Rubisco enzyme.

The reduction of AQY, J_{max} and Φ_{PSII} in *linho* compared to WT, suggested a detrimental effect of mutation on the light energy conversion processes and the rate at which absorbed excitation energy can be dissipated by PSII photochemistry. Especially, the reduced Φ_{PSII} indicated an alteration of PSII reaction centers, which inevitably reduces the maximum flux of electrons through the photosynthetic electron-transport chain. In barley plants, it has been hypothesized that SA can have a direct effect on the photosynthetic electron chain, decreasing the number of PSII centers and disturbing the redox cycling of the rest operative water-oxidizing centers (Maslenkova et al., 2009). The transmembrane protein PsbX, associated with the oxygen-evolving complex, appears to be involved in the regulation of the amount of PSII and may be implicated in the binding

or turnover of quinone molecules at the Qb (PsbA) site (Shi et al., 2012). It has been shown the reduction of PsbX contents in *Arabidopsis* antisense plants leads to reduced levels of functional assembled PSII core complexes of about 30-40%, suggesting that PsbX is important for accumulation of functional PSII (García-Cerdán et al., 2008). Hence, the down-regulation of the *HaPsbX* gene in *linho* mutant could indicate a lower amount of functional PSII centers, leading to a reduced photochemistry activity and electron transport rate capacity.

4.4. Effects of mutation on the dissipation of excessive light and energy balance

The reduced electron transport rate in *linho* was associated with an increased light energy pressure at PSII, as suggested by the enhanced $1\text{-}q_p$ values. Anyway, NPQ and $1\text{-}F_{v'}/F_{m'}$, which furnish an estimation of thermal energy dissipation capacity, were only slightly affected in *linho* compared to WT at growth light intensity. To evaluate possible alteration in the energy dissipation mechanism under increasing radiative pressure, we compared the light-response curves of Φ_{PSII}, $1\text{-}q_p$ and NPQ in *linho* and WT plants. As expected, the increase of light irradiance caused a reduction of Φ_{PSII} associated with an increase of $1\text{-}q_p$ and NPQ in both mutant and WT. However, *linho* showed higher $1\text{-}q_p$ values at saturating light intensity associated with lower NPQ and $1\text{-}F_{v'}/F_{m'}$ values with respect to WT, suggesting a reduced capacity in dissipating the excess light energy as heat (Demmig-Adams et al., 1996; Müller et al., 2001). Accordingly, light response curves of NPQ in tobacco leaf segments infiltrated with 2 mM SA indicated a limited capacity to regulate excess energy dissipation, especially at high light irradiance when the reduced rate of electron transport may contribute to explain the decreased NPQ (Janda et al., 2012). These authors hypothesized that SA could alter NPQ kinetics affecting ΔpH build-up and/or reducing the rate of zeaxanthin formation. This xanthophyll component is produced from de-epoxidation of violaxanthin to zeaxanthin through the violaxanthin de-epoxidase enzyme and is involved in NPQ (Farber et al.,

1997). However, our data showed that the expression of the *Violaxanthin de-epoxidase* gene *(HaVDE*) was not statistically affected by mutation, while the expression of *Phytoene synthase* gene (*HaPSY*) in *linho* was down-regulated. Hence, these data suggested a depression of the transcriptional activity of genes involved in the first steps of the carotenogenic pathway. Moreover, the gene expression of the *Photosystem II 22 kDa protein* (*HaPsbS*) was strongly down-regulated in *linho* respect to WT. The PsbS protein is localized in PSII super-complexes and is directly involved in the light activation of NPQ (Correa-Galvis et al., 2016). Therefore, the reduced thermal dissipation capacity at saturating light intensity in *linho* could be due to a lower amount of both carotenoid compounds and HaPsbS protein at PSII level. According to this hypothesis, the light response curve of NPQ in transgenic tobacco plants with a reduced *HaPsbS* expression showed a higher Q_A redox state associated with lower NPQ at increasing light irradiance (Glowacka et al., 2018). The excess light energy that is neither used for photosynthetic electron transport rate nor dissipated as heat may lead to an overreduction of PSII and, finally, to photoinhibition (Kato et al., 2003). It has been shown as moderate photoinhibition of PSII leads to a stimulation of cyclic electron flow at low light. The enzyme ferredoxin $NADP^+$ reductase (FNR) has been suggested to provide a possible docking site for ferredoxin regulating the electron flow around photosystem I to increase ATP synthesis, possibly facilitating the rapid repair of photodamaged PSII (Huang et al., 2018). Interestingly, the gene expression of *HaFNR* was not significantly different in *linho* leaves with respect to WT, suggesting that this crucial pathway was not affected by mutation.

The inhibition of photosynthesis in *linho* was associated with changes in the respiratory metabolism, with an increased R_L/R_D ratio at vegetative stage and a higher R_D at reproductive stage than WT. Dahl et al. (2017) suggested that, under conditions limiting the photosynthetic metabolism, a coordinated regulation of photosynthetic and respiratory components is necessary to maintain chloroplast energy balance in varied growth conditions. In particular, these authors showed that under drought conditions and high irradiance the alternative oxidase amount became a crucial determinant of R_L, contributing to maintain chloroplast energy balance and photosynthetic

performance. Moreover, Hou et al. (2018) indicated that the alternative respiratory pathway and SA could mediate the H_2O_2-induced acclimation of PSII to excess light. Mateo et al. (2006) observed an increase of R_D, associated with a reduced photosynthetic activity on *Arabidopsis* mutants showing constitutively high SA levels. Therefore, we can hypothesize that stimulation of the respiratory metabolism could contribute to counteract the increase in PSII excitation pressure and to compensate the energy imbalance in leaves of *linho* with high SA/SAG ratio.

5. Conclusions

This work suggests an inhibitory effect of high leaf SA/SAG ratio on the photosynthetic metabolism of *linho* under optimal growth conditions. The altered photosynthetic capacity in *linho* was due to a combination of stomatal and non-stomatal limitations. Especially, our data show that the reduced carboxylation efficiency and PSII functionality were associated with a down-regulation of the related gene expression. In addition, *linho* exhibited a stimulation of respiration, suggesting a coordinate modulation of photosynthetic and respiratory metabolism. Although we cannot exclude a possible direct effect of the mutation on the energy conversion processes, our data suggest a possible regulatory role of SA/SAG ratio on the energy balance of this mutant. The effects of controlled endogenous SA levels on the regulation of energy balance and cellular redox homeostasis could be dependent on the light conditions (Mateo et al., 2006). Hence, further studies will be necessary to evaluate how the acclimation at different light intensity affects growth, photosynthesis and respiration in *linho*. This information could be essential to unravel the interactions among SA metabolism, light acclimation and energy conversion processes in the higher plants under non-stress conditions.

CrediT author statement

Andrea Scartazza, Marco Fambrini, Lorenzo Mariotti, Piero Picciarelli, Claudio Pugliesi: Conceptualization, Methodology, Validation, Formal Analysis, Investigation, Data Curation, Writing – Original Draft, Writing – Review & Editing.

Declaration of competing interest

None

Acknowledgements

This study was funded by the Special Fund 2018-2019 of the University of Pisa. The funders had no role in study design, data collection and analysis, decision to publish or preparation of the manuscript.

References

Andersson, I., 2008. Catalysis and regulation in Rubisco. J. Exp. Bot. 5, 1555-1568. https://doi.org/10.1093/jxb/ern091

Bernacchi, C.J., Singsaas, E.L., Pimentel, C., Portis, A.R. Jr, Long, S.P., 2001. Improved temperature response functions for models of Rubisco-limited photosynthesis. Plant Cell Environ. 24, 253-259. https://doi.org/10.1111/j.1365-3040.2001.00668.x

Bernacchi, C.J., Pimentel, C., Long, S.P., 2003. *In vivo* temperature response functions of parameters required to model RuBP-limited photosynthesis. Plant Cell Environ. 26, 1419-1430. https://doi.org/10.1046/j.0016-8025.2003.01050.x

Çag, S., Cevahir-Öz, G., Sarsag, M., Gören-Saglam, N., 2009. Effect of salicylic acid on pigment, protein content and peroxidase activity in excised sunflower cotyledons. Pak. J. Bot. 41, 2297-2303

Correa-Galvis, V., Poschmann, G., Melzer, M., Stühler, K., Jahns, P., 2016. PsbS interactions involved in the activation of energy dissipation in *Arabidopsis*. Nature Plants 2, 15225. https://doi.org/10.1038/nplants.2015.225

Dahal, K., Martyn, G.D., Alber, N.A., Vanlerberghe, G.C., 2017. Coordinated regulation of photosynthetic and respiratory components is necessary to maintain chloroplast energy balance in varied growth conditions. J. Exp. Bot. 68, 657-671. https://doi.org/10.1093/jxb/erw469

Dean, J.V., Mills, J.D., 2004. Uptake of salicylic acid 2- O- β- D- glucose into soybean tonoplast vesicles by an ATP- binding cassette transporter- type mechanism. Physiol. Plant. 120, 603-612. https://doi.org/10.1111/j.0031-9317.2004.0263.x

Demmig- Adams, B., Adams III, W.W., Barker, D.H., Logan, B.A., Bowling, D.R., Verhoeven, A.S., 1996. Using chlorophyll fluorescence to assess the fraction of absorbed light allocated

to thermal dissipation of excess excitation. Physiol. Plant. 98, 253-264. https://doi.org/10.1034/j.1399-3054.1996.980206.x

Dogra, V., Kim, C., 2019. Chloroplast protein homeostasis is coupled with retrograde signaling. Plant Signal Behav. https://doi: 10.1080/15592324.2019.1656037

Fambrini, M., Castagna, A., Dalla Vecchia, F., Degl'Innocenti, E., Ranieri, A., Vernieri, P., Pardossi, A., Guidi, L., Rascio, N., Pugliesi, C., 2004. Characterization of a pigment-deficient mutant of sunflower (*Helianthus annuus* L.) with abnormal chloroplast biogenesis, reduced PS II activity and low endogenous level of abscisic acid. Plant Sci. 167, 79-89. https://doi.org/10.1016/j.plantsci.2004.03.002

Farber, A., Young, A.J., Ruban, A.V., Horton, P., Jahns, P., 1997. Dynamics of xanthophyll-cycle activity in different antenna subcomplexes in the photosynthetic membranes of higher plants. The relationship between zeaxanthin conversion and nonphotochemical fluorescence quenching. Plant Physiol., 115, 1609-1618. https://doi.org/10.1104/pp.115.4.1609

Fariduddin, Q., Hayat, S., Ahmad, A., 2003. Salicylic acid influences net photosynthetic rate, carboxylation efficiency, nitrate reductase activity, and seed yield in *Brassica juncea*. Photosynthetica 41, 281-284. https://doi.org/10.1023/B:PHOT.0000011962.05991.6c

Farquhar, G.D., von Caemmerer, S.V., Berry, J.A., 1980. A biochemical model of photosynthetic CO_2 assimilation in leaves of C 3 species. Planta 149, 78-90. https://doi.org/10.1007/BF00386231

Foyer, C.H., Neukermans, J., Queval, G., Noctor, G., Harbinson, J., 2012. Photosynthetic control of electron transport and the regulation of gene expression. J. Exp. Bot. 63, 1637-1661. https://doi.org/10.1093/jxb/ers013

Gao, Y., Liu, W., Wang, X., Yang, L., Han, S., Chen, S., Strasser, R.J., Valverde, B.E., Qiang, S., 2018. Comparative phytotoxicity of usnic acid, salicylic acid, cinnamic acid and benzoic acid on photosynthetic apparatus of *Chlamydomonas reinhardtii*. Plant Physiol. Biochem. 128, 1-12. https://doi: 10.1016/j.plaphy.2018.04.037

García-Cerdán, J.G., Sveshnikov, D., Dewez, D., Jansson, S., Funk, C., Schröder, W.P., 2008. Antisense inhibition of the PsbX protein affects PSII integrity in the higher plant *Arabidopsis thaliana*. Plant Cell Physiol. 50, 191-202. https://doi.org/10.1093/pcp/pcn188

Genty, B., Briantais, J.M., Baker, N.R., 1989. The relationship between the quantum yield of photosynthetic electron transport and quenching of chlorophyll fluorescence. Biochim. Biophys. Acta Gen. Subj. 990, 87-92. https://doi.org/10.1016/S0304-4165(89)80016-9

Gonzalez-Bayon, R., Shen, Y., Groszmann, M., Zhu, A., Wang, A., Allu, A.D., Dennis, E.S., Peacock, W.J., Greaves, I.K., 2019. Senescence and defense pathways contribute to heterosis. Plant Physiol. 180, 240-252. https://doi: 10.1104/pp.18.01205

Głowacka, K., Kromdijk, J., Kucera, K., Xie, J., Cavanagh, A.P., Leonelli, L., Leakey, A.D.B., Ort, D.R., Niyogi, K.K., Long, S.P., 2018. Photosystem II subunit S overexpression increases the efficiency of water use in a field-grown crop. Nat. Commun. 9, 868. https://doi.org/10.1038/s41467-018-03231-x

Groszmann, M., Gonzalez-Bayon, R., Lyons, R.L., Greaves, I.K., Kazan, K., Peacock, W.J., Dennis, E.S., 2015. Hormone-regulated defense and stress response networks contribute to heterosis in *Arabidopsis* F1 hybrids. Proc. Natl. Acad. Sci. USA 112, E6397-E6406. https:// doi: 10.1073/pnas.1519926112

Habibi, G., Vaziri, A., 2017. High salicylic acid concentration alters the electron flow associated with photosystem II in barley. Acta Agric. Slov. 109, 393-402. http://dx.doi.org/10.14720/aas.2017.109.2.22

Handa, N., Kohli, S.K., Kaur, R., Khanna, K., Bakshi, P., Thukral, A.K., Arora, S., Ohri, P., Mir, B.A., Bhardwaj, R., 2017. Emerging trends in physiological and biochemical responses of salicylic acid. In: R. Nazar et al. (Eds.), Salicylic Acid: A Multifaceted Hormone. Springer Nature Singapore Pte Ltd., pp. 47-75 https://doi.org/10.1007/978-981-10-6068-7_4

Robards, A.W., 1978. An introduction to techniques for scanning electron microscopy of plant cells. In: Hall, J.L. (Ed.), Electron Microscopy and Cytochemistry of Plant Cells. Elsevier, New York, pp. 343-403.

Hou, Q.Z., Wang, Y.P., Liang, J.Y., Jia, L.Y., Feng, H.Q., Wen, J., Ehmet, N., Bai, J.Y., 2018. H_2O_2-induced acclimation of photosystem II to excess light is mediated by alternative respiratory pathway and salicylic acid. Photosynthetica 56, 1154-1160. http://doi.org/10.1007/s11099-018-0806-8

Huang, W., Yang, Y.J., Zhang, S.B., Liu, T., 2018. Cyclic electron flow around photosystem I promotes ATP synthesis possibly helping the rapid repair of photodamaged photosystem II at low light. Front. Plant Sci. 9, 239. htpp://doi.org/10.3389/fpls.2018.00239

Janda, T., Gondor, O.K., Yordanova, R., Szalai, G., Pál, M., 2014. Salicylic acid and photosynthesis: signalling and effects. Acta Physiol. Plant. 36, 2537-2546.

Janda, K., Hideg, É., Szalai, G., Kovács, L., Janda, T., 2012. Salicylic acid may indirectly influence the photosynthetic electron transport. J. Plant Physiol. 169, 971-978. https://doi.org/10.1016/j.jplph.2012.02.020

Kato, M.C., Hikosaka, K., Hirotsu, N., Makino, A., Hirose, T., 2003. The excess light energy that is neither utilized in photosynthesis nor dissipated by photoprotective mechanisms determines the rate of photoinactivation in photosystem II. Plant Cell Physiol. 44, 318-325. https://doi.org/10.1093/pcp/pcg045

Kok, B., 1948. A critical consideration of the quantum yield of *Chorella* photosynthesis. Enzymologia 13, 1-56.

Kumar, D., 2014. Salicylic acid signaling in disease resistance. Plant Sci. 228, 127-134. https://doi.org/10.1016/j.plantsci.2014.04.014

Kumazaki, A., Suzuki, N., 2019. Enhanced tolerance to a combination of heat stress and drought in Arabidopsis plants deficient in ICS1 is associated with modulation of photosynthetic reaction center proteins. Physiol. Plant. 165, 232-246. https:// doi:10.1111/ppl.12809

Levine, R.P., 1969. The analysis of photosynthesis using mutant strains of algae and higher plants. Annu. Rev. Plant. Physiol. 20, 523-540. https://doi.org/10.1146/annurev.pp.20.060169.002515

Livak, K.J., Schmittgen, T.D., 2001. Analysis of relative gene expression data using real-time quantitative PCR and the $2^{-\Delta\Delta C_T}$ method. Methods 25, 402-408. https://doi.org/10.1006/meth.2001.1262

Lu, Y., Yao, J., 2018. Chloroplasts at the crossroad of photosynthesis, pathogen infection and plant defense. Int. J. Plant Sci. 19, 3900. https://doi.org/10.3390/ijms19123900

Maruri-López, I., Aviles-Baltazar, N.Y., Buchala, A., Serrano, M. 2019. Intra and extracellular journey of the phytohormone salicylic acid. Front. Plant Sci. 10, 423. https://doi.org/10.3389/fpls.2019.00423

Maslenkova, L., Peeva, V., Stojnova, Z., Popova, L., 2009. Salicylic acid-induced changes in photosystem II reactions in barley plants. Biotechnol. Biotechnol. Equip. 23, 297-300. https://doi.org/10.1080/13102818.2009.10818423

Mariotti, L., Fambrini, M., Scartazza, A., Picciarelli, P., Pugliesi, C., 2018. Characterization of *lingering hope*, a new brachytic mutant in sunflower (*Helianthus annuus* L.) with altered salicylic acid metabolism. J. Plant Physiol. 231, 402-414. https://doi.org/10.1016/j.jplph.2018.10.020

Mateo, A., Funck, D., Mühlenbock, P., Kular, B., Mullineaux, P.M., Karpinski, S., 2006. Controlled levels of salicylic acid are required for optimal photosynthesis and redox homeostasis. J. Exp. Bot. 57, 1795-1807. https://doi.org/10.1093/jxb/erj196

Müller, P., Li, X.P., Niyogi, K.K., 2001. Non-photochemical quenching. A response to excess light energy. Plant Physiol. 125, 1558-1566. https://doi.org/10.1104/pp.125.4.1558

Pancheva, T.V., Popova, L.P., Uzunova, A.N., 1996. Effects of salicylic acid on growth and photosynthesis in barley plants. J. Plant. Physiol. 149, 57-63. https://doi.org/10.1016/S0176-1617(96)80173-8

Pancheva, T.V., Popova, L.P., 1998. Effect of salicylic acid on the synthesis of ribulose-1, 5-bisphosphate carboxylase/oxygenase in barley leaves. J. Plant Physiol. 152, 381-386. https://doi.org/10.1016/S0176-1617(98)80251-4

Poór, P., Borbély, P., Bódi, N., Bagyánski, M., 2019. Effects of salicylic acid on photosynthetic activity and chloroplast morphology under light and prolonged darkness. Photosynthetica 57, 367-376. https://doi.org/10.32615/ps.2019.040

Portis, Jr. A.R., Li, C., Wang, D., Salvucci, M.E., 2007. Regulation of Rubisco activase and its interaction with Rubisco. J. Exp. Bot. 59, 1597-1604. https://doi.org/10.1093/jxb/erm240

Rivas-San Vicente, M., Plasencia, J., 2011. Salicylic acid beyond defence: its role in plant growth and development. J. Exp. Bot. 62, 3321-3338. https://doi.org/10.1093/jxb/err031

Rochaix, J.D., 2004. Genetics of the biogenesis and dynamics of the photosynthetic machinery in eukaryotes. Plant Cell 16, 1650-1660. https://doi.org/10.1105/tpc.160770

Scartazza, A., Picciarelli, P., Mariotti, L., Curadi, M., Barsanti, L., Gualtieri, P., 2017. The role of *Euglena gracilis* paramylon in modulating xylem hormone levels, photosynthesis and water-use efficiency in *Solanum lycopersicum* L. Physiol. Plant. 161, 486-501. https://doi.org/10.1111/ppl.12611

Schneiter, A.A., Miller, J.F., 1981. Description of sunflower growth stages. Crop Sci. 21, 901-903. https://doi.org/10.2135/cropsci1981.0011183X002100060024x

Shi, L.X., Hall, M., Funk, C., Schröder, W.P., 2012. Photosystem II, a growing complex: updates on newly discovered components and low molecular mass proteins. Biochim. Biophys. Acta Gen. Subj. 1817, 13-25. https://doi.org/10.1016/j.bbabio.2011.08.008

Slattery, R.A., Van Loocke, A., Bernacchi, C.J., Zhu, X.G., Ort, D.R., 2017. Photosynthesis, light use efficiency, and yield of reduced-chlorophyll soybean mutants in field conditions. Front. Plant Sci. 8, 549. https://doi.org/10.3389/fpls.2017.00549

Thorneycroft, D., Sherson, S.M., Smith, S.M., 2001. Using gene knockouts to investigate plant metabolism. J. Exp. Bot. 361, 1593-1601. https://doi.org/10.1093/jexbot/52.361.1593

Uzunova, A.N., Popova, L.P., 2000. Effect of salicylic acid on leaf anatomy and chloroplast ultrastructure of barley plants. Photosynthetica 38, 243-250. https://doi.org/10.1023/A:1007226116925

Wang, Y.Y, Wang, Y., Li, G.Z., Hao, L., 2019. Salicylic acid-altering Arabidopsis plant response to cadmium exposure: Underlying mechanisms affecting antioxidation and photosynthesis-related processes. Ecotoxicol. Environ. Saf. 169, 645-653. https://doi: 10.1016/j.ecoenv.2018.11.062

Wu, L., Zu, X., Wang, X., Sun, A., Zhang, J., Wang, S., Chen, Y., 2013. Comparative proteomic analysis of the effects of salicylic acid and abscisic acid on maize (*Zea mays* L.) leaves. Plant Mol. Biol. Rep. 31, 507-516. https://doi.org/10.1007/s11105-012-0522-7

Xue, L.J., Guo, W., Yuan, Y., Anino, E.O., Nyamdari, B., Wilson, M.C., Frost, C.J., Chen, H.-Y., Babst, B.A., Harding, S.A., Tsai, C.J., 2013. Constitutively elevated salicylic acid levels alter photosynthesis and oxidative state but not growth in transgenic populus. Plant Cell 25, 2714-2730. https://doi.org/10.1105/tpc.113.112839

Zhang, Y., Li, X., 2019. Salicylic acid: biosynthesis, perception, and contributions to plant immunity. Curr. Opin. Plant Biol. 50, 29-36. https://doi.org/10.1016/j.pbi.2019.02.004

Figure legends

Fig. 1. Leaf content of free salicylic acid (SA) and of the conjugate SA 2-O-β-D-glucoside (SAG) in the second pair of leaves of wild type (WT) and *lingering hope* (*linho*) mutant plants of sunflower (*Helianthus annuus* L.). Data are means ± SE from three independent experiments, with run in triplicates (plants). The insert shows the SA/SAG ratio in WT and *linho*. *** Significantly different from WT at the $P < 0.01$ level according to a Student's *t*-test.

Fig. 2. Photosynthetic response of CO_2 assimilation rate (A) to increasing photosynthetic photon flux density (PPFD) in the second pair of leaves of wild type (WT) and *lingering hope* (*linho*) mutant plants of sunflower (*Helianthus annuus* L.). Data are means ± SE from three independent experiments, with run in triplicates (plants).

Fig. 3. Photosynthetic response of CO_2 assimilation rate (A) to increasing intercellular CO_2 concentration (C_i) in the second pair of leaves of wild type (WT) and *lingering hope* (*linho*) mutant plants of sunflower (*Helianthus annuus* L.) at saturating light intensity (1800 μmol m^{-2} s^{-1}). Data are means ± SE from three independent experiments, with run in triplicates (plants).

Fig. 4. Light response curves of (A) effective quantum yield of PSII photochemistry (Φ_{PSII}), (B) radiative pressure at PSII ($1-q_p$) and (C) non-photochemical quenching (NPQ) in the second pair of leaves of wild type (WT) and *lingering hope* (*linho*) mutant plants of sunflower (*Helianthus annuus* L.) at saturating light intensity (1800 μmol m^{-2} s^{-1}). Data are means ± SE from three independent experiments, with run in triplicates (plants).

Fig. 5. Expression level of photosynthetic-related genes in the second pair of leaves of wild type (WT) and *lingering hope* (*linho*) mutant plants of sunflower (*Helianthus annuus* L.). (A) *Rubisco*

large subunit (*HaRbcL*); (B) *Rubisco small subunit* (*HaRbcS*); (C) *Rubisco activase* (*HaRbcA*); (D) *photosystem II PsbX* (*HaPsbX*); (E) *Photosystem II 22 kDa protein* (*HaPsbS*); (F) *Photosystem I chlorophyll a/b-binding protein 3-1,* chloroplastic (*HaLhcA*); (G) *Ferredoxin-NADP*$^{+}$ *reductase* (*HaFNR*); (H) *Phytoene synthase* (*HaPSY*); (I) *Violaxanthin de-epoxidase* (*HaVDE*). Data are means ± SD of three/four biological replicates. Ns not significant; *, ** Significantly different from WT at the $P < 0.05$ and $P < 0.01$ level according to a Student's *t*-test, respectively.

Supplementary materials

Table S1 List of genes from sunflower (*Helianthus annuus* L.) analyzed and gene-specific primers used for real-time RT-PCR (RT-qPCR).

CrediT author statement

Andrea Scartazza, Marco Fambrini, Lorenzo Mariotti, Piero Picciarelli, Claudio Pugliesi: Conceptualization, Methodology, Validation, Formal Analysis, Investigation, Data Curation, Writing – Original Draft, Writing – Review & Editing.

Table 1

Pigments contents, photosynthetic performance and respiratory fluxes in the second pair of leaves of 21-days-old plants of wild type (WT) and *lingering hope* (*linho*) mutant of sunflower (*Helianthus annuus* L.) grown under 200 μmol m^{-2} s^{-1}. Data are means ± SE from three independent experiments, with run in triplicates (plants). Ns not significant. *, **, *** Significantly different from WT at the $P < 0.05$, $P < 0.01$ and $P < 0.001$ level according to a Student's *t*-test, respectively.

Parameter	WT	*linho*	*P level*
Leaf pigments			
Chl *a* (μg mg^{-1} FW)	1.444 ± 0.099	0.966 ± 0.088	*
Chl *b* (μg mg^{-1} FW)	0.424 ± 0.027	0.263 ± 0.023	*
Chl *a+b* (μg mg^{-1} FW)	1.868 ± 0.126	1.229 ± 0.111	*
Car (μg mg^{-1} FW)	0.294 ± 0.018	0.246 ± 0.021	Ns
Gas Exchange			
A (μmol m^{-2} s^{-1})	8.75 ± 0.22	5.94 ± 0.21	***
$\mathbf{g_s}$ (mol m^{-2} s^{-1})	0.368 ± 0.031	0.266 ± 0.019	*
$\mathbf{C_i}$ (μmol mol^{-1})	334 ± 4	337 ± 5	Ns
E (mmol m^{-2} s^{-1})	4.51 ± 0.34	3.73 ± 0.25	*
Fluorescence of Chl a			
$\mathbf{F_v/F_m}$	0.815 ± 0.005	0.757 ± 0.011	**
$\mathbf{\Phi_{PSII}}$	0.704 ± 0.012	0.601 ± 0.018	***
$\mathbf{1\text{-}q_p}$	0.080 ± 0.005	0.145 ± 0.010	***
NPQ	0.23 ± 0.03	0.27 ± 0.03	Ns
$\mathbf{1\text{-}F_{v'}/F_{m'}}$	0.24 ± 0.02	0.27 ± 0.02	Ns
Light-response curve			
$\mathbf{A_{max}}$ (μmol m^{-2} s^{-1})	30.9 ± 2.7	21.4 ± 1.6	***
AQY (μmol μmol^{-1})	0.062 ± 0.002	0.050 ± 0.003	***
LCP (μmol mol^{-1})	31.0 ± 6.6	36.8 ± 8.0	Ns
Θ	0.60 ± 0.07	0.59 ± 0.02	Ns
$\mathbf{\Phi_{PSII\text{-}SAT}}$	0.367 ± 0.026	0.213 ± 0.014	***
$\mathbf{1\text{-}q_{p\text{-}SAT}}$	0.518 ± 0.010	0.744 ± 0.016	***
$\mathbf{NPQ_{SAT}}$	1.41 ± 0.15	0.61 ± 0.06	***
$\mathbf{1\text{-}F_{v'}/F_{m'\text{-}SAT}}$	0.49 ± 0.02	0.42 ± 0.02	*
CO_2 response curve			
$\mathbf{V_{cmax}}$ (μmol m^{-2} s^{-1})	142.9 ± 15.0	103.2 ± 11.2	***
$\mathbf{J_{max}}$ (μmol m^{-2} s^{-1})	265.2 ± 25.6	187.9 ± 20.0	***
$\mathbf{J_{max}/V_{cmax}}$	1.86 ± 0.06	1.82 ± 0.06	Ns
CCP (μmol mol^{-1})	42.7 ± 1.8	46.2 ± 1.1	Ns
Respiratory fluxes			
$\mathbf{R_D}$ (μmol m^{-2} s^{-1})	2.05 ± 0.22	1.97 ± 0.28	Ns
$\mathbf{R_L}$ (μmol m^{-2} s^{-1})	1.15 ± 0.09	1.67 ± 0.22	*
$\mathbf{R_L/R_D}$	0.58 ± 0.05	0.85 ± 0.03	*

Table 2

Pigments content, gas exchanges, chlorophyll fluorescence and respiration in the dark in the leaves of 11°-12° internode in 70-days-old plants of both wild type (WT) and *lingering hope* (*linho*) mutant of sunflower (*Helianthus annuus* L.) grown under 200 μmol m^{-2} s^{-1}. Gas exchange and fluorescence measurements were carried out at both growth and saturating light intensity. Values of F_v/F_m and R_D were obtained after 30 min of acclimation to dark. Data are means ± SE from three independent experiments, with run in triplicates (plants). Ns not significant. *, **, *** Significantly different from WT at the $P < 0.05$, $P < 0.01$ and $P < 0.001$ level according to a Student's *t*-test, respectively.

Parameter	**WT**	***linho***	***P* level**
Leaf pigments			
Chl *a* (μg mg^{-1} FW)	1.26 ± 0.08	0.77 ± 0.13	***
Chl *b* (μg mg^{-1} FW)	0.36 ± 0.01	0.22 ± 0.02	***
Chl *a+b* (μg mg^{-1} FW)	1.63 ± 0.06	0.99 ± 0.07	***
Car (μg mg^{-1} FW)	0.31 ± 0.01	0.20 ± 0.01	***
Growth light intensity (PPFD 200 μmol m^{-2} s^{-1})			
A (μmol m^{-2} s^{-1})	9.18 ± 0.38	5.25 ± 0.49	***
g_s (mol m^{-2} s^{-1})	0.195 ± 0.022	0.140 ± 0.012	*
C_i (μmol mol^{-1})	287.3 ± 16.3	322.2 ± 6.8	*
E (mmol m^{-2} s^{-1})	2.77 ± 0.28	2.11 ± 0.15	*
Φ_{PSII}	0.709 ± 0.005	0.527 ± 0.032	***
1-q_p	0.071 ± 0.003	0.290 ± 0.038	***
NPQ	0.21 ± 0.04	0.19 ± 0.03	Ns
1-$F_{v'}/F_{m'}$	0.24 ± 0.01	0.26 ± 0.01	Ns
Saturating light intensity (PPFD 1800 μmol m-2 s-1)			
A (μmol m^{-2} s^{-1})	20.74 ± 1.09	9.71 ± 0.09	***
g_s (mol m^{-2} s^{-1})	0.209 ± 0.017	0.142 ± 0.014	**
C_i (μmol mol^{-1})	209.0 ± 8.2	267.8 ± 13.1	**
E (mmol m^{-2} s^{-1})	3.36 ± 0.27	2.39 ± 0.20	**
Φ_{PSII}	0.199 ± 0.009	0.092 ± 0.010	***
1-q_p	0.644 ± 0.017	0.856 ± 0.016	***
NPQ	1.36 ± 0.10	0.64 ± 0.09	***
1-$F_{v'}/F_{m'}$	0.44 ± 0.01	0.36 ± 0.01	**
Dark-adapted leaves			
F_v/F_m	0.805 ± 0.002	0.775 ± 0.006	***
R_D (μmol m^{-2} s^{-1})	1.22 ± 0.08	2.04 ± 0.13	***

Figure 1

Click here to download high resolution image

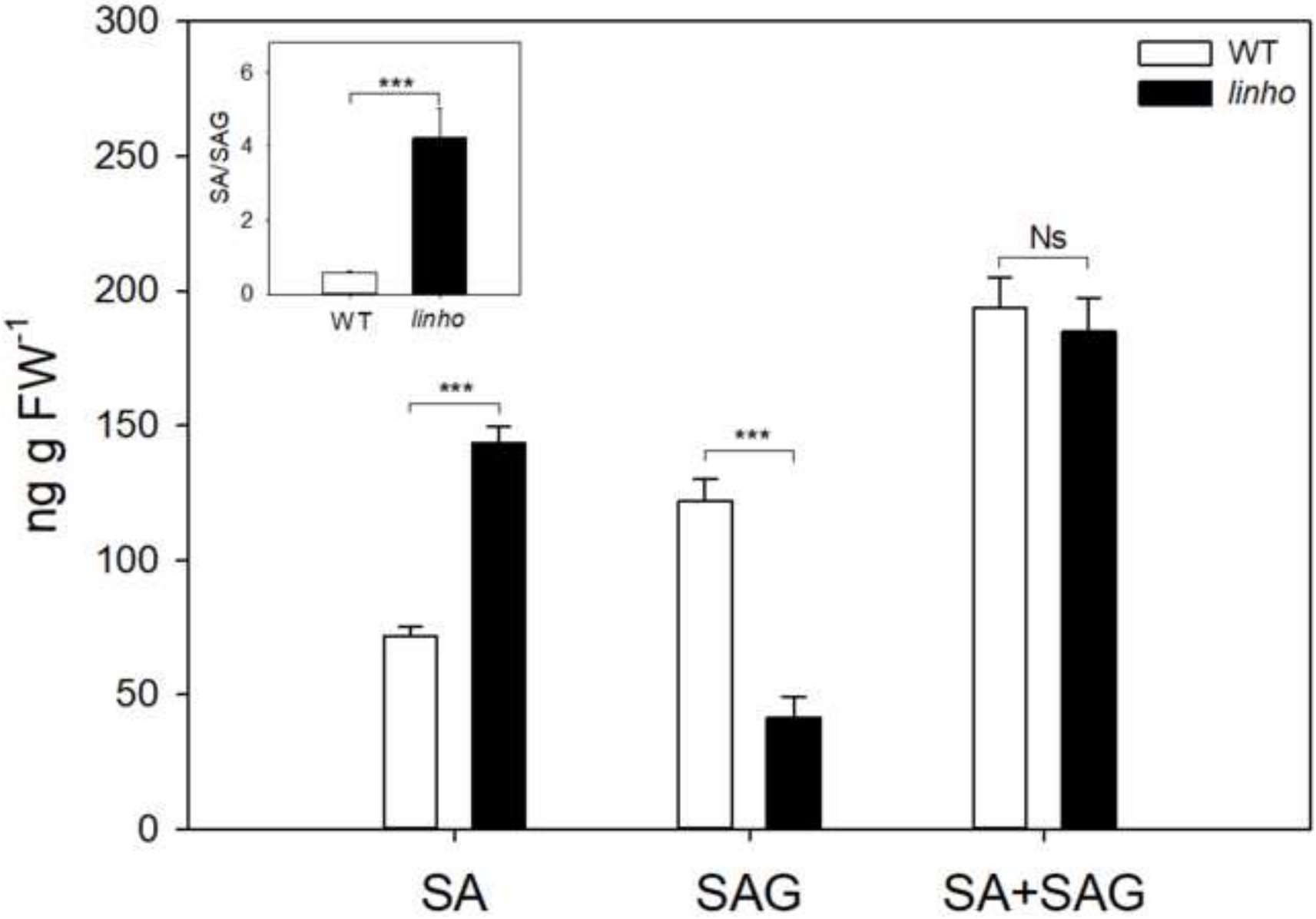

Fig. 1

Figure 2
Click here to download high resolution image

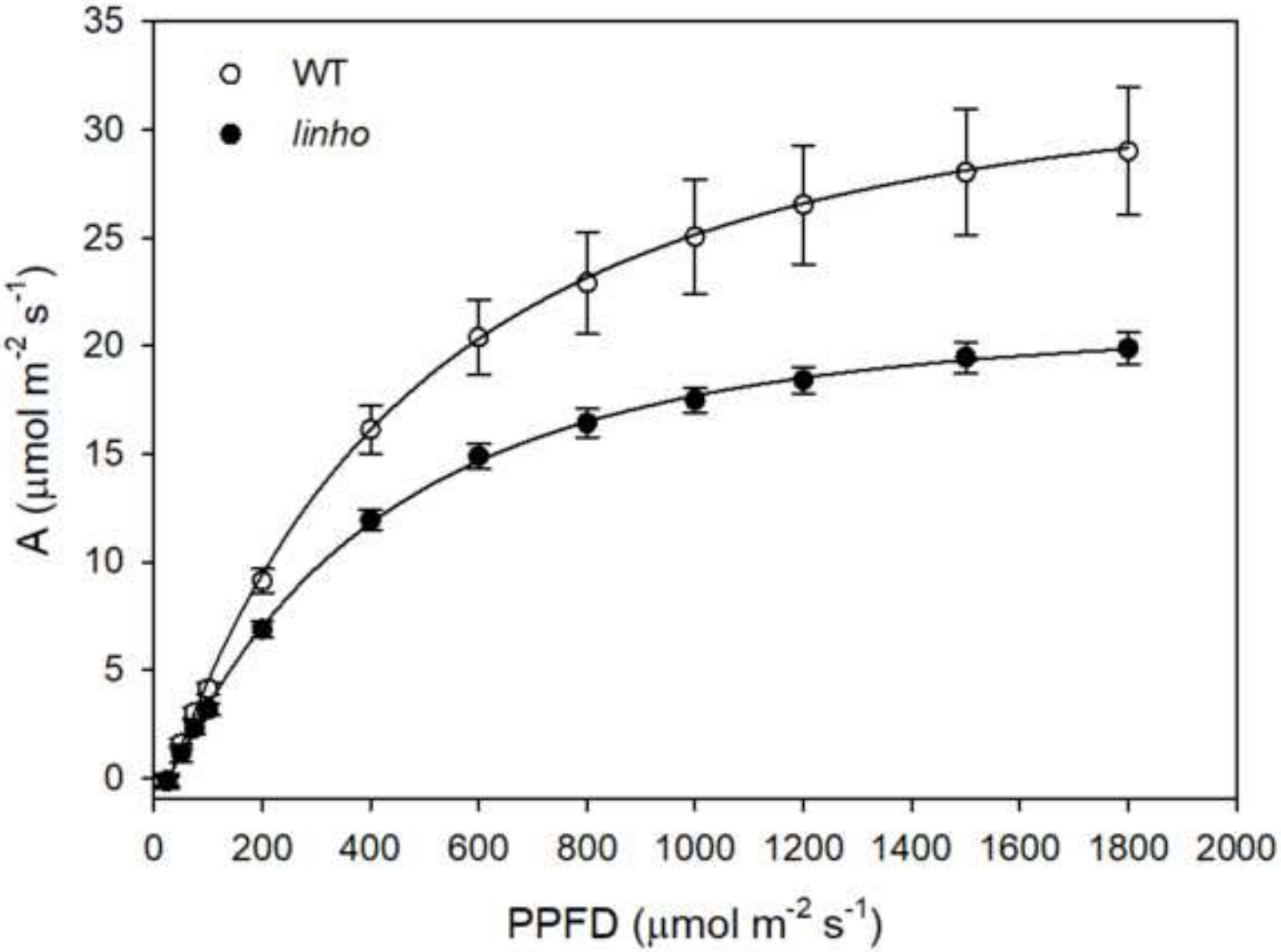

Fig. 2

Figure 3
Click here to download high resolution image

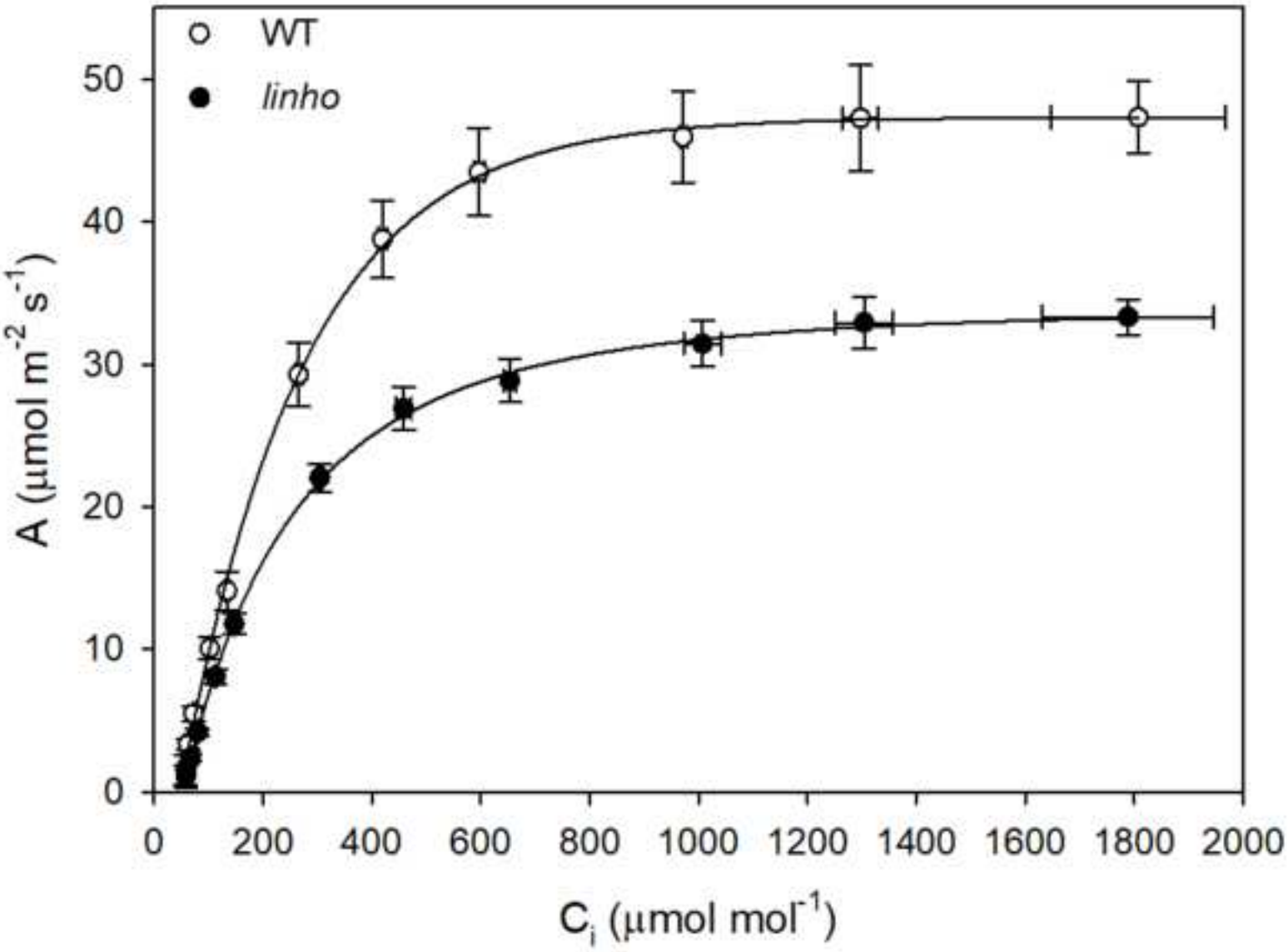

Fig. 3

Figure 4

Click here to download high resolution image

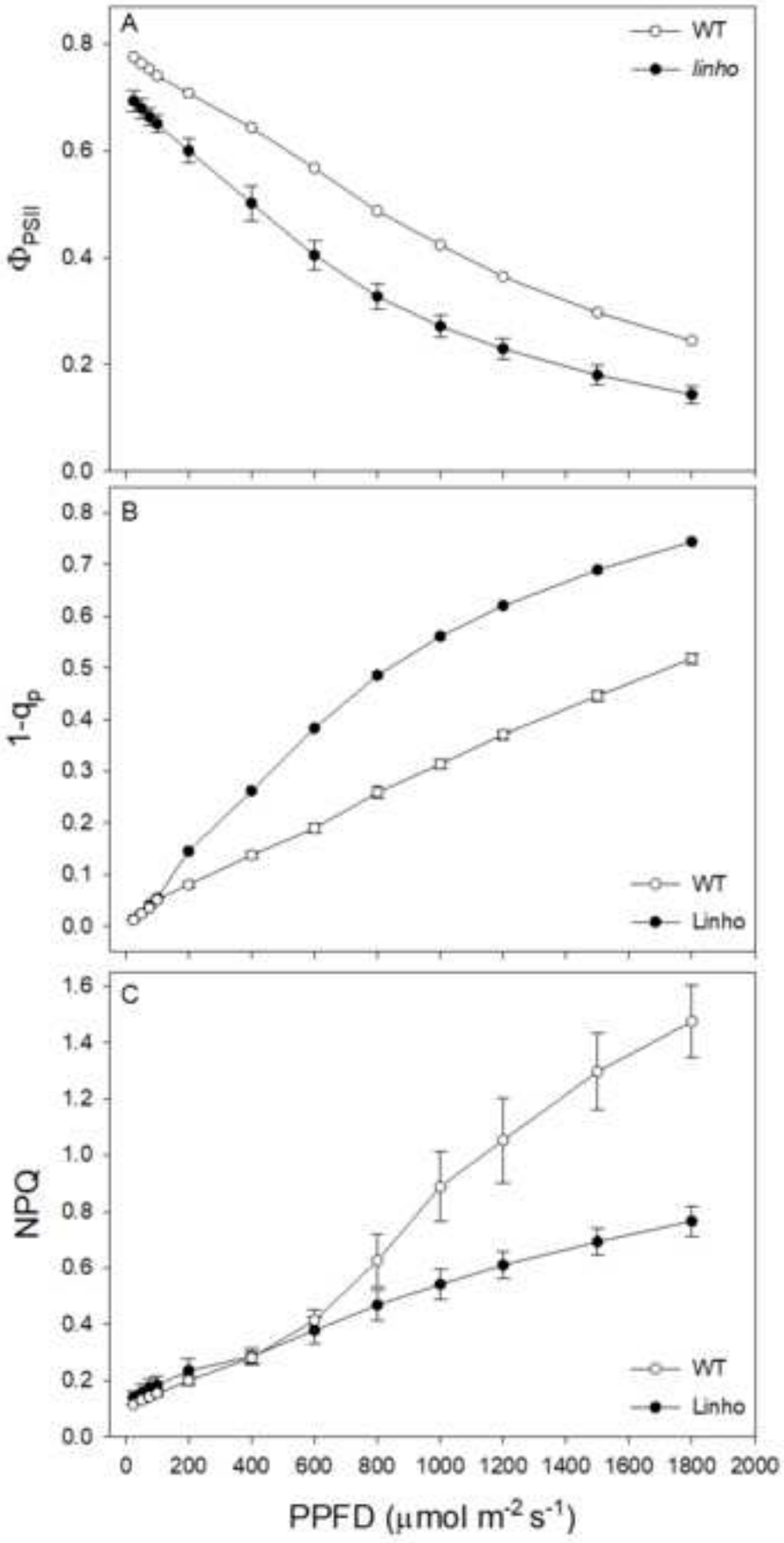

Fig. 4

Figure 5

Click here to download high resolution image

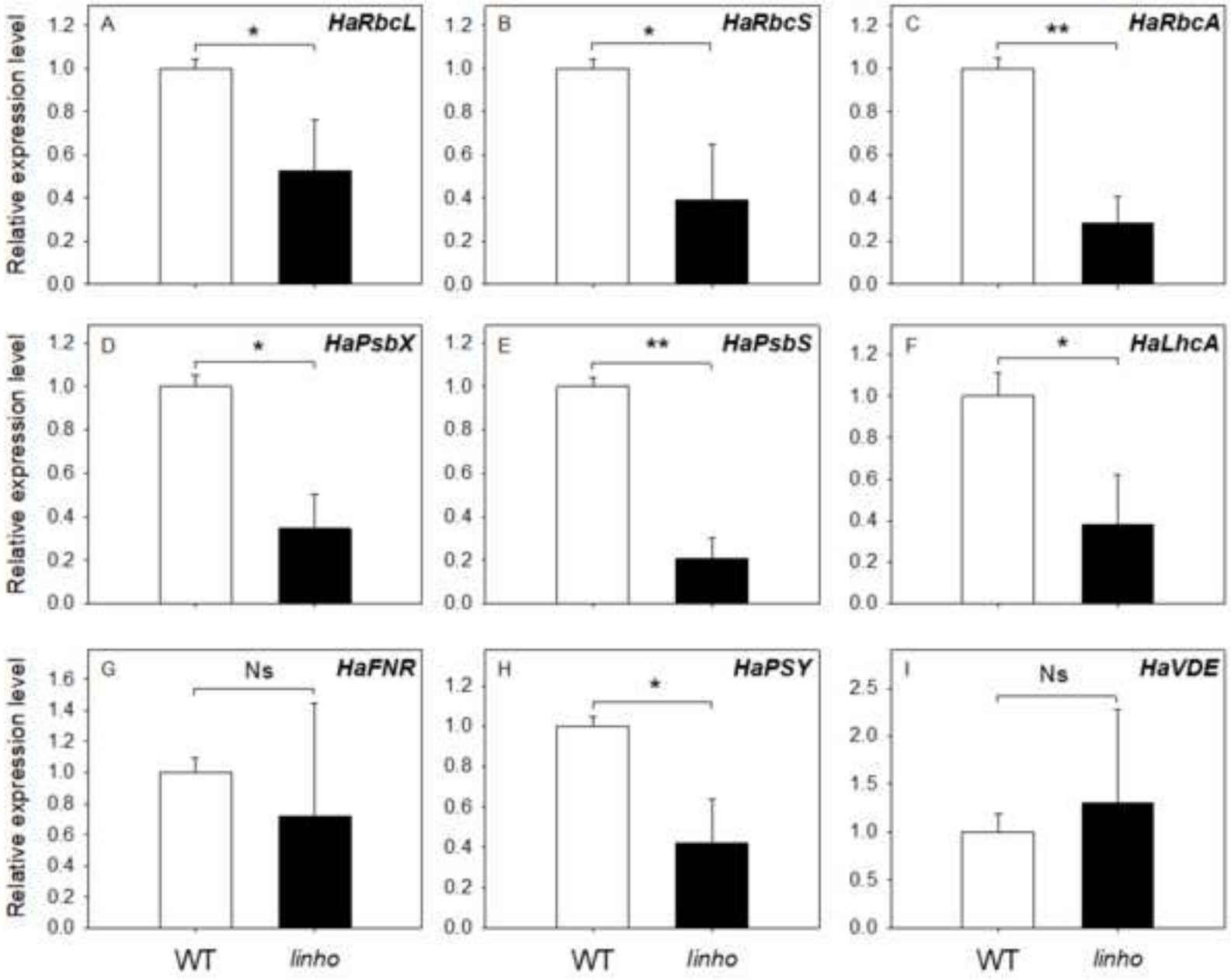

Fig.5

Supplementary material

Click here to download Supplementary material: Supplementary material Table S1.docx

***Declaration of Interest Statement**

Declaration of interests

☒ The authors declare that they have no known competing financial interests or personal relationships that could have appeared to influence the work reported in this paper.

☐The authors declare the following financial interests/personal relationships which may be considered as potential competing interests: